PHILOSOPHICAL TRANSACTIONS OF THE ROYAL SOCIETY A MATHEMATICAL, PHYSICAL & ENGINEERING SCIENCES

Muonium Dynamics in Semiconductors

R. L. Lichti

Phil. Trans. R. Soc. Lond. A 1995 **350**, 323-333
doi: 10.1098/rsta.1995.0018

Muonium dynamics in semiconductors

By R. L. Lichti

Physics Department, Texas Tech University, Lubbock, Texas 79409, U.S.A.

Investigations of the dynamics of muonium transitions in semiconductors using RF-μSR and longitudinal depolarization measurements are described. Results for intrinsic and doped Si allow development of an essentially complete model for the Mu dynamics. Energy barriers are compared with the few available measurements for H in Si. In intrinsic and p-type samples three states, Mu^0_{BC}, Mu^0_T, and Mu^+_{BC} are active and at high temperatures a rapid cycle among all three states is identified. In n-type samples the Mu^-_T state becomes important and numerous additional transitions become active. Parameters are extracted for seven separate transition processes and features associated with several additional ones are identified. Preliminary data for other materials are also briefly discussed.

1. Introduction

Hydrogen enters most semiconductors quite easily either during crystal growth or during various processing steps. It is chemically active in these materials forming complexes with donor or acceptor dopants and interacting with various other defects to modify electrical and optical properties relevant to device performance. Understanding the dynamics of hydrogen related reactions in semiconductor materials is thus very important. However, observation of isolated hydrogen is difficult and most of the information on isolated H behaviour is from study of H-related complexes, or inferred from measurements of material properties which are modified by formation or break up of such complexes. Investigation of the light short-lived pseudo-isotope muonium Mu= (μ^+,e^-) has been extremely successful in elucidating the structures and static properties of isolated H (Paterson 1988; Kiefl & Estle 1990), and was especially important is helping to establish the bond-centred site as the lowest energy state for the neutral isolated H defect centre (Kiefl *et al.* 1988).

Over the last several years an international collaboration has been investigating the site and charge-state changes of Mu in semiconductors, concentrating primarily on silicon. We have used methods with applied fields parallel to the initial muon polarization, specifically a driven muon-spin-resonance technique known as RF-μSR and longitudinal-field (LF) depolarization measurements, which are far more sensitive to final states than conventional transverse-field (TF) μSR techniques due to removal of precessional phase coherence requirements. A combination of RF-μSR and LF data on a series of doped Si samples ranging in concentration from roughly 10^{15} cm^{-3} p-type to 10^{16} cm^{-3} n-type coupled with theoretical considerations have allowed development of an essentially complete dynamic model describing transitions among the various Mu states. We discuss

Phil. Trans. R. Soc. Lond. A (1995) **350**, 323–333
Printed in Great Britain

the basic features observed in these investigations and our assignments of the transitions responsible for each. The dynamic parameters we obtain for Mu are compared to the few analogous measurements for H and the applicability of the muonium dynamic results to hydrogen behaviour in silicon is assessed. Preliminary results for other materials are very briefly discussed.

Early TF time-differential (TD) μSR data (Patterson 1988) identified three spectra for positive muons implanted in Si, as well as most other tetrahedrally bonded semiconductors: an isotropic paramagnetic centre known as Mu, an anisotropic paramagnetic centre known as Mu* and a non-paramagnetic centre known either as the *diamagnetic* or μ^+ signal. Further investigations eventually identified the Mu* signal as arising from a neutral defect with the μ^+ residing at the centre of a stretched bond (Kiefl *et al.* 1988; Estle *et al.* 1986, 1987; Estreicher 1987). The unpaired e^- is in a non-bonding orbital with most of the spin density on the two nearest neighbours. This is the lower energy state of the two neutral centres in Si. The metastable neutral, the isotropic Mu state, is rapidly diffusing among the tetrahedral interstitial regions in the lattice. The diamagnetic state can be either a bare μ^+ or have two e^- associated with it, i.e. either a Mu^+ or Mu^- ion in chemical terminology. Here we use a notation which identifies both the site and charge state: thus, Mu is labelled as Mu^0_T and the Mu* centre becomes Mu^0_{BC}. Theoretical results imply that the positive charge state will be stable at the BC-site, Mu^+_{BC}, and that the negative ionic state will only occur as a T-site species, Mu^-_T (Myers *et al.* 1992).

2. Longitudinal depolarization processes

For sufficiently high conduction electron density n_e, interactions of the Mu^0 states with electrons lead to depolarization of the muon spin. Two types of interactions are important and lead to very similar experimental results. At high temperatures a rapid e^- capture/ionization charge cycle is observed in the LF data on all semiconductors examined to date (Chow *et al.* 1993; Lichti *et al.* 1994*a*). At lower temperatures spin-exchange scattering of conduction electrons from Mu^0 is observed (Chow *et al.* 1994*b*). For either charge or spin exchange, the muon spin depolarization is a result of random changes in the M_S quantum state of the neutral muonium centre's electron which are transmitted to the muon via hyperfine interactions. The depolarization rates measured in an LF experiment are specifically sensitive to the charge or spin exchange rates and the hyperfine frequency of the neutral state involved. A full field and temperature dependence allows extraction of the appropriate rate parameters and the Mu^0 hyperfine parameters.

LF identification of Mu^0 states. Under conditions of sufficiently slow spin-flip scattering or charge exchange the field dependence for the two neutral centres is very different and serves as a quick state identification (Chow *et al.* 1994*b*). The isotropic Mu^0_T shows a constant rate at low fields and drops off as B^{-2} at high fields, while the anisotropic Mu^0_{BC} has a sharp peak at a well defined field given by $B_P = (A_\perp \sin^2\theta + A_\parallel \cos^2\theta)/2\gamma_\mu$, where the As are the hyperfine parameters, γ_μ is the muon gyromagnetic ratio, and θ is the angle between the applied field and the $\langle 1\,1\,1\rangle$ bond axis. At this field the parallel component of the net internal field goes to zero for $M_S = +1/2$ leading to maximum mixing of the muon spin states due to oscillations in the perpendicular effective field.

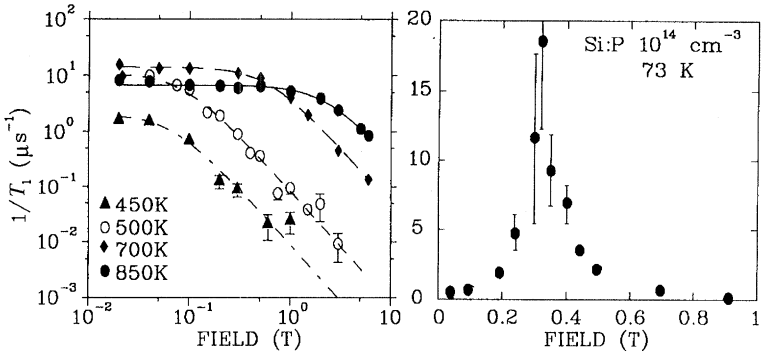

Figure 1. Longitudinal depolarization rates as a function of field illustrating features used to identify the Mu^0 state. (*a*) Data from the high-temperature charge cycle in intrinsic Si, characteristic of the isotropic Mu^0_T state. (*b*) Data for spin-exchange scattering from Mu^0_{BC} in the N14 sample. The peak is characteristic of an anisotropic centre at slow exchange rates.

Figure 1 displays the field dependent LF relaxation data typical of each of the Mu^0 centres. The lower temperature data in figure 1*b* are for the spin-exchange scattering process involving Mu^0_{BC}. The high temperature data in figure 1*a* are for the cyclic charge exchange involving Mu^0_T as the neutral state. The displayed field dependences identify the Mu^0 state while the process identification relies on additional information regarding ionization and capture rates from TFTD and RF-μSR data. For rapid exchange rates compared to the hyperfine frequency both neutral centres give curves which are qualitatively similar to the isotropic result at low rates, and a full fit is necessary to make a state identification based solely on the hyperfine parameter.

The high-temperature charge-exchange cycle. The hyperfine frequency required to fit the data in figure 1*a*, along with similar curves at a few other temperatures seals the identification of Mu^0_T as the relaxing species in near intrinsic Si (Chow *et al.* 1993). Our preliminary fits of these data were based on a two state model involving a +/0 Mu charge cycle and gave an ionization energy of 0.34(1) eV with a capture cross section of $2.8(3) \times 10^{-15}$ cm^2. Decay positron channelling data (Simmler *et al.* 1992). identify only a near-BC site from roughly 270 to 400 K where TFTD μSR data only show the μ^+ signal. Coupled with theory, these results clearly imply a Mu^+_{BC} state at the onset of this charge cycle. One must conclude that a BC to T site change is necessary just above 400 K in intrinsic Si for all of these results to be satisfied. The RF results discussed below are consistent with this conclusion, and the high temperature LF relaxation data are currently being reexamined with an extended model including more complicated options combining charge and site changes.

We have examined high-purity Ge and several samples of semi-insulating and doped GaAs (Lichti *et al.* 1994*a*) in addition to both intrinsic (Chow *et al.* 1993) and doped (Chow *et al.* 1994*a*) silicon. These combined results indicate that the cyclic charge exchange is definitely an *electron* exchange process since the onset temperatures shift with the e^- density. In each of these materials muon depolarization due to the charge cycle starts at essentially identical e^- capture rates (Lichti *et al.* 1994*a*). For the intrinsic or semi-insulating materials the onset scales appropriately with the gap energy, i.e. the wider the gap the higher the charge cycle onset temperature. In the doped materials the onset shifts to lower tem-

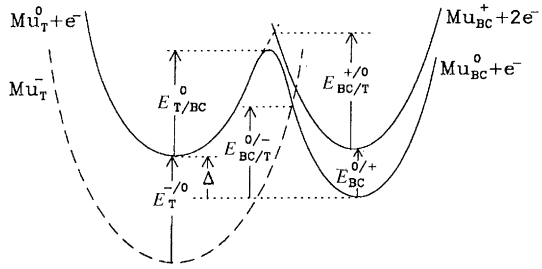

Figure 2. Idealized configuration diagram for Mu in silicon: states are Mu^0_{BC} and Mu^+_{BC} (right) and Mu^0_T and Mu^-_T (left). Three particles, the μ^+ and two e^-, are included. For intrinsic and p-type samples the second e^- and the Mu^-_T state can be ignored.

peratures for n-type and to higher temperatures for p-type at moderate doping levels. In sufficiently highly doped n-type materials the onsets are suppressed by nearly 100% occupation of the Mu^- state even to quite high temperatures when the e^- capture rates are much greater than the ionization rates. Study of materials other than Si is at a relative early stage and the measurements required to identify the responsible Mu^0 states have been scheduled.

3. Dynamic model for Mu in Si

Data from our recent dynamic investigations have been interpreted in terms of a model which considers transitions among the four possible Mu states: Mu^0_{BC}, Mu^0_T, Mu^+_{BC}, and in n-type materials Mu^-_T. Figure 2 is an idealized configuation diagram which describes this model and defines the various energy parameters. In labelling transitions and associated parameters we use a sub- or superscript showing the initial/final site or charge state respectively. We do not consider any transitions which require a double charge transfer, and eliminate transitions with obviously higher barriers than competing paths out of a given state. We have used a three-state theoretical model which yields an analytic solution when important transitions are included. The more complete four-state model has not yet been fully worked out; however, we have managed to experimentally determine which of the ionic states contributes to the diamagnetic signal in most cases. We have used the simplest rate expressions consistent with our understanding of each process. For simple ionizations and site changes rates are of the form $\nu = \rho_0 e^{-E/kT}$; for simple carrier capture the rates are $\nu = nv\sigma$; and for combined site changes and carrier capture the cross section is replaced by an activated total-process cross section $\sigma = \sigma_0 \exp(-E/kT)$.

Thus far we have obtained dynamic parameters associated with seven processes and identify features associated with an eighth in the RF-μSR data. Low temperature LF data have helped sort out the transition assignments, particularly in the n-type materials. The high temperature cyclic charge exchange leads to loss of all RF signals and only the onset region is accessible via RF experiments. We have examined the temperature dependences of the time-integral intensity of the three μSR spectra under RF excitation in a total of ten silicon samples. Several previous reports presented preliminary results on the near intrinsic and p-type samples (Lichti *et al.* 1992; Hitti *et al.* 1994; Lichti *et al.* 1994*b*). For the present

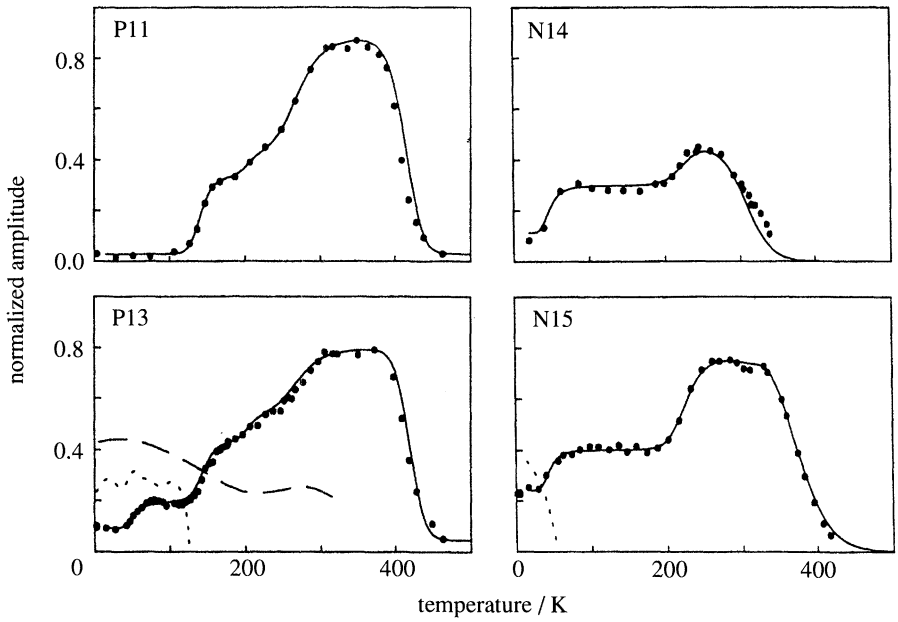

Figure 3. RF-μSR data for selected p- and n-type Si samples. Features related to each important transition process are represented. Most quoted parameters are from fits to samples P11 and N15. Data points are the diamagnetic signal, either Mu^{+}_{BC} or Mu^{-}_{T}, the dotted line is Mu^{0}_{BC}, and the dashed curve is Mu^{0}_{T}.

paper discussion of specific data will be limited to only a few the ten samples actually examined, but will show the general features associated with nearly all transition processes.

Figure 3 shows the RF-μSR results for four Si samples which together display all of the relevant features: (*a*) P11 is p-type with a net doping level of $3.0\times10^{11}\,\mathrm{cm}^{-3}$, (*b*) P13 is doped at $1.0\times10^{13}\,\mathrm{cm}^{-3}$; while the other two are more heavily doped n-type samples, (*c*) N14 at $4.9\times10^{14}\,\mathrm{cm}^{-3}$, and (*d*) N15 at $1.5\times10^{15}\,\mathrm{cm}^{-3}$. The fits shown use parameters which yield an overall fit to the whole series of samples. The relevant parameters are shown in table 1, along with the associated transition processes. Energies were obtained from P11 and N15 with prefactors averaged from best fits to individual samples to produce a compromise fit which is satisfactory across the full doping range. In the n-type samples the diamagnetic signal is a combination of both the $Mu^{\pm}$ ionic states and we used the relative rates for various transitions to assign the dominant ionic state as a function of temperature. Similar rate comparisons were used to check consistency of our process assignments. The overall model holds together extremely well, with only a few isolated crossover regions still preliminary. The following details the assignment of specific features in both RF-μSR and LF relaxation data. A more complete description of the RF-μSR experimental techniques and analysis and discussion of the full data set is being published elsewhere (Kreitzman *et al.* 1994).

The P11 sample is the most nearly intrinsic one of this set. At low temperatures the two Mu^{0} states are populated in roughly equal amounts consistent with TFTD results (Patterson 1988). The step in the diamagnetic signal (data points in the figure) at 140 K is due to ionization of Mu^{0}_{BC} to Mu^{+}_{BC} as seen at this temperature

Table 1. *Transition processes identified for Mu in silicon along with the associated RF-μSR feature used in fitting and the resulting dynamic parameters*

transition process	RF feature		parameters
BC charge-state transitions:			
$Mu^0_{BC} \rightarrow Mu^+_{BC} + e^-$	P11	140 K	$\rho^{0/+}_{BC} = 3.1 \times 10^{13}\ s^{-1}$
			$E^{0/+}_{BC} = 0.22 \pm 0.01$ eV
$Mu^0_{BC} + h^+ \rightarrow Mu^+_{BC}$	P13	50 K	$\sigma^{0/+}_{BC} = 2.0 \times 10^{-15}\ cm^2$
$Mu^+_{BC} + e^- \rightarrow Mu^0_{BC}$	N13		$\sigma^{+/0}_{BC} = 1.0 \times 10^{-15}\ cm^2$
T charge-state transitions:			
$Mu^0_T + e^- \rightarrow Mu^-_T$	N15	50 K	$\sigma^{0/-}_{T} = 0.8 \times 10^{-15}\ cm^2$
$Mu^-_T \rightarrow Mu^0_T + e^-$	N15	300 K	$(E^{-/0}_T)$
site-change transitions:			
$Mu^0_T \rightarrow Mu^0_{BC}$	P11	270 K	$\rho^{0}_{T/BC} = 9.5 \times 10^{12}\ s^{-1}$
			$E^{0}_{T/BC} = 0.39 \pm 0.04$ eV
$Mu^+_{BC} + e^- \rightarrow Mu^0_T$	P11	400 K	$\sigma_0 = 1.2 \times 10^{-10}\ cm^2$
			$E^{+/0}_{BC/T} = 0.38 \pm 0.06$ eV
	N15	340 K	$\rho^{+/0}_{BC/T} = 3.0 \times 10^{11}\ s^{-1}$
			$E^{+/0}_{BC/T} = 0.40 \pm 0.02$ eV
$Mu^0_{BC} + e^- \rightarrow Mu^-_T$	N15	200 K	$\rho^{0/-}_{BC/T} = 1.6 \times 10^{13}\ s^{-1}$
			$E^{0/-}_{BC/T} = 0.34 \pm 0.01$ eV
interactions with dopants:			
$Mu^0_T + A^0 \rightarrow Mu^+_{BC} + A^-$	P	$T = 0$	
$Mu^0_T + D^0 \rightarrow Mu^-_T + D^+$	N	$T = 0$	

in the increase of T_2^{-1} relaxation rates from the TFTD data. Parameters from the earlier measurements do a good job simulating this step; however, the present data provide a complete set of independent parameters and yield a somewhat higher ionization energy of $E^{0/+}_{BC} = 0.22(1)$ eV, which locates the BC(+/0) level relative to the conduction band edge, compared to 0.17(1) eV from the TFTD results. Since the parent state is anisotropic the small feature just above 200 K is also from this process, representing the delayed observation of spin components perpendicular to the effective local fields. Listed errors are statistical; simulations suggest that real errors are larger, probably between 10 and 15% for all energies.

The broader step centred around 270 K represents ionization of Mu^0_T in a two step process ending with Mu^+_{BC}. The rate limiting step is assigned to a $Mu^0_T \rightarrow Mu^0_{BC}$ site change from the metastable to stable Mu^0 confguration, which is

PHILOSOPHICAL TRANSACTIONS OF THE ROYAL SOCIETY A MATHEMATICAL, PHYSICAL & ENGINEERING SCIENCES

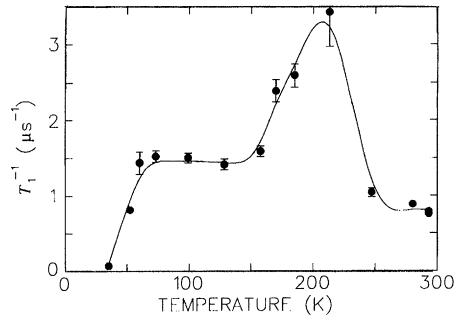

Figure 4. Temperature dependent longitudinal depolarization rates for N14 used to help identify states and transition processes in n-type Si.

rapidly followed by the thermal promotion of the e^- to the conduction band. The site-change barrier is found to be $E^0_{T/BC} = 0.39(4)$ eV. The drop in the RF diamagnetic intensity starting at about 400 K is the signature of the onset of the rapid charge exchange process. To fit the steepness of this drop, it was necessary to use an activated capture process implying a combined site change and e^- capture. This is fully consistent with a RT state of Mu^+_{BC} and an active high-temperature relaxing state of Mu^0_T as inferred from the LF data discussed above. The barrier obtained from P11 for this combined site and charge state transition is $E^{+/0}_{BC/T} = 0.38(6)$ eV.

The B-doped p-type samples all show the above features, with the P13 data (figure 3*b*) demonstrating additional features at low temperatures related to dopants. The step at roughly 50 K is due to ionization of the acceptor and subsequent capture of a hole by Mu^0_{BC} to form Mu^+_{BC}. The increased diamagnetic signal at very low temperatures represents an interaction between the mobile Mu^0_T and acceptors at very short times, perhaps during thermalization of the implanted muon. Some form of charge exchange reaction either forms Mu^+_{BC} and B^- or a Mu–B pair if the muon is trapped next to the B-site (Myers *et al.* 1992). These two features grow with increasing p-type dopant concentration and the 50 K step appropriately shifts in temperature with the dopant acceptor level energy when Ga or In replace B. None of the p-type samples show any hint of a Mu^- ionic state at any temperature.

The Mu dynamics in n-type Si are much more complicated due to the added Mu^-_T state. Here we show two of the more highly doped samples to illustrate the important features. Below roughly 200 K the Mu^+_{BC} state is not observed in any of the n-type samples. This is likely because of depolarization of the BC fraction of the signal due to spin and/or charge exchange even at rather low e^- densities. In intrinsic Si the high temperature charge exchange begins when n_e reaches roughly 10^{13} cm^{-3}. Longitudinal relaxation data hold the key to understanding much of the n-type behaviour. Figure 4 displays the temperature dependent rate constant for the relaxing component in N14. A peak above RT (not shown) is from the high temperature cyclic process involving Mu^+_{BC} and Mu^0_T. Below 200 K all of the relaxing component has been identified as arising from Mu^0_{BC} by the observed field dependence. Note that in N15 the RF signal from this state disappears rapidly near 50 K as seen in figure 3*d*.

Combined RF and LF data on N14 provide the following assignments. At 50 K the P donors ionize and an electron is subsequently captured by Mu^0_T to form

Mu_T^- in a process strictly analogous to the 50 K step in the p-type samples. Accompanying this donor ionization the spin-exchange scattering process causes an increase in the LF relaxation rate. The field dependence proves that this scattering is from the Mu_{BC}^0 state which is still present even though the RF-μSR signal from that state is rapidly broadened by the depolarization process and disappears above 50 K. The thermal ionization of Mu_{BC}^0 still occurs just as in the p-type samples, although perhaps shifted to slightly higher temperatures. It is observed as an increase in LF relaxation rate around 160 K. The increased depolarization above the BC ionization temperature is due to a cyclic e^- capture/ionization at the BC-site switching between Mu_{BC}^+ and Mu_{BC}^0. Essentially none of the initial BC fraction is seen in the RF data on N14 between 50 K and 200 K due to these interactions with conduction electrons. For lighter n-type doping the same trends are seen, although some portion of the BC signals remain visible in the RF data. An accurate modelling of these data will require a full treatment of all four Mu states, including the depolarization and transition processes; which is well beyond our current analytic three-state model.

Near 200 K in all of the n-type samples a rather abrupt increase is seen in the diamagnetic intensity. This has been assigned to an activated e^- capture leading from Mu_{BC}^0 to Mu_T^-. Our best data on this process is for N15, where a fit yields an energy barrier of $E_{BC/T}^{0/-} = 0.34(1)$ eV. We have confirmed that the rate for this path out of Mu_{BC}^0 begins to exceed the depolarization rate from the BC charge cycle at roughly this temperature. Therefore, above 200 K the initial BC fraction becomes visible in the diamagnetic RF-μSR signal as Mu_T^-. For N15 and higher doped samples essentially all of the of the T-site species are in the Mu^- charge state between 50 and 300 K.

Just above room temperature in N15 the second e^- is thermally promoted to the conduction band, and the rapid transition rates for processes already discussed drive the system to Mu_{BC}^+ and then into the high-temperature combined charge/site cycle. Our present identifications and rate parameters imply that this cycle is the same for all of our samples. The small dip in the diamagnetic intensity just above 300K in N15 may be due to a $0/-$ charge cycle at the T-site; however, this feature overlaps the second anisotropy step from the 200 K BC$\rightarrow$T site change and we have been unable to extract any dynamic information. This electron loss barrier would give the final energy parameter needed to complete our dynamic model, the T$(0/-)$ level position below the conduction band edge. A slightly different dopant concentration or a differently oriented sample may make this feature accessible, completing the picture. The absence of thermal e^- loss from Mu_T^- up to RT implies that the T$(0/-)$ level is quite deep, consistent with arguments that H and Mu form negative-U centres in Si.

Comparison with hydrogen data. Several measurements on the E3′ DLTS line (Holm *et al.* 1991; Bech-Nielsen *et al.* 1994) and the AA9 EPR centre (Gorelkinski & Nevinnyi 1992; Bech-Nielsen *et al.* 1994) both assigned to H_{BC}^0 provide the main comparison data between Mu and H dynamics in Si. The E3′ DLTS energy is 0.164(11) eV (Holm *et al.* 1991) for the hydrogen BC$(+/0)$ donor level depth. The corresponding Mu number is 0.168(13) eV from the TFTD data or 0.22(1) eV from our RF data. The latter error is underestimated based on simulations. Theoretical expectations are that strictly electronic energy differences should be nearly identical for H and Mu.

The other two available comparisons are for the processes we identify as acti-

PHILOSOPHICAL TRANSACTIONS OF THE ROYAL SOCIETY A MATHEMATICAL, PHYSICAL & ENGINEERING SCIENCES

vated e^- capture, going from the BC to T site in both cases. The H barriers are from isochronal annealing studies on a time scale roughly 8 orders of magnitude longer than the Mu experiments. For the $H^+_{BC} \rightarrow H^0_T$ transition the barrier is 0.44(1) eV from the DLTS work (Holm *et al.* 1991) and 0.48(4) eV from the EPR data (Gorelkinski & Nevinnyi 1992). Our result yields $E^{+/0}_{BC/T} = 0.40(2)$ eV from a fit to the high-temperature charge-cycle onset in N15 and 0.38(6) eV for the same feature in P11. This energy difference is in the direction expected for site changes when one takes into account the larger kinetic energy of the muon compared to a proton. The other energy obtained is $E^{0/-}_{BC/T} = 0.34(1)$ eV from the 200 K step in N15. The comparable $H^0_{BC} \rightarrow H^-_T$ barrier is 0.293(3) eV for ^{1}H and 0.30(1) eV for ^{2}H from the DLTS annealing curves (Holm *et al.* 1991). We expect the Mu result to be somewhat too high because the depolarization processes will skew the RF data; thus, again these numbers appear to be in reasonable agreement. Considering the expected differences and the experimental complications, this comparison strongly suggests that experiments on muonium dynamics in semiconductors can yield a very good model for isolated hydrogen behaviour. Given the difficulty in directly observing isolated H impurities, the Mu results should be highly relevant to anyone trying to model hydrogen diffusion and passivation or dissociation reactions. At the very least, the muonium data strongly imply that models which assume a single H state in most situations need to be reexamined since a complicated set of site and charge-state transitions are active on quite short time scales compared with any of the H experiments.

4. Preliminary data for GaAs

We have examined several n-type GaAs samples in low longitudinal fields to measure the depolarization rates. These samples show a considerable amount of sample dependence which appears to go beyond what may be expected from concentration differences. Intrinsic defects and various compensating impurities are quite likely active in these samples, interacting with each other and muonium. Nevertheless, a considerable amount of information can be gleaned from these preliminary data, always with the understanding that some of the features may move around or disappear in similar samples. Figure 5 shows the LF relaxation rates in a particularly clean sample where the features appear to correspond to earlier TFTD data. This is a GaAs(Si) sample doped at about 3×10^{15} cm^{-3} which is well below the metallic level. These data were fit as two components, one relaxing and the other non-relaxing. In general any ionic charge state will be non-relaxing and the T-site neutral should relax much more rapidly than the BC counterpart because of the difference in hyperfine parameters. The peak in rate constant near 600 K is assigned to the high-temperature charge cycle, although the states involved have not been identified. The onset is slightly shifted downward in temperature from earlier data obtained in semi-insulating GaAs (Lichti *et al.* 1994*a*) again confirming an electron exchange process. The lower temperature data show a change in rate centred around 200 K. This is accompanied by an amplitude change from the non-relaxing to relaxing components, which is strongly suggestive of a transition into the T site. This would be consistent with theoretical results which place the T-site with Ga near neighbours as the neutral ground state in GaAs (Myers *et al.* 1992). Two other features in the amplitudes (not shown) appear consistent with other knowledge of Mu behaviour in GaAs:

PHILOSOPHICAL TRANSACTIONS OF THE ROYAL SOCIETY A MATHEMATICAL, PHYSICAL & ENGINEERING SCIENCES

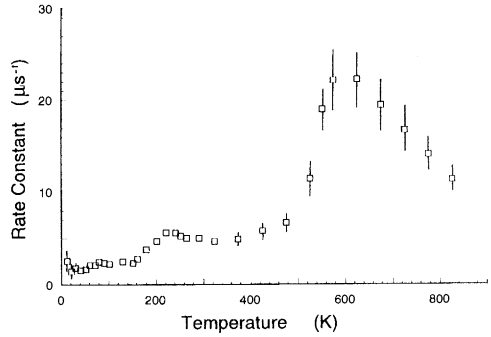

Figure 5. Temperature dependent longitudinal depolarization rates for the relaxing fraction in n-type GaAs(Si) doped at approximately 10^{15} cm^{-3}.

a small peak in the non-relaxing amplitude occurs near the Mu^0_T ionization as seen around 250 K in TFTD data (Patterson 1988), and below 40 K there is a large transfer from non-relaxing to the relaxing component fully consistent with ionization of the shallow Si donors. Considerably more work is required in GaAs before state identifications are verified and sample dependent aspects of Mu dynamics are sorted out.

The motional stability of both Mu^+ and Mu^- have been studied in metallic n-type samples of GaAs(Si), GaAs(Te) and in p-type GaAs(Zn). Preliminary results indicate that Mu^- is very stable and does not show motional narrowing until roughly 500 K, while Mu^+ shows motion begining at about 200 K. In the case of Mu^+, which should be in a near BC position but more strongly bound to one host atom (Myers *et al.* 1992) the motion is most likely local hopping among the four equivalent bonds around a common central atom. There is some indication of additional motion for Mu^+ in the neighbourhood of 500 K, which is most likely global diffusion. Additional data will be required to extract accurate barriers in each case. The trends observed in GaAs appear to be consistent with theoretical results and the changes in stability of various sites due to the partial ionicity of the GaAs host material. Investigations of trends with III–V ionicity would help clarify these effects.

5. Conclusions

Investigations of the dynamics of Mu in silicon are nearing completion and have led to an essentially complete dynamic model involving all four states expected to play any role. The energy parameters obtained from our RF-μSR and longitudinal depolarization studies of intrinsic and doped Si compare quite favorably with the few existing analogous numbers for hydrogen. The overall model developed from the muonium work should be applicable to hydrogen dynamics when zero-point kinetic energy effects are properly taken into account. The model we have developed also provides a basis for evaluating developing theoretical efforts to treat dynamic processes involving impurities in semiconductors. Because the muonium data imply that a quite complicated series of site and charge-state changes are active, especially in n-type materials, models of hydrogen diffusive behaviour which assume a single active state should be reexamined. Preliminary data for GaAs suggest that the dynamics of Mu in several other materials may

PHILOSOPHICAL TRANSACTIONS OF THE ROYAL SOCIETY A MATHEMATICAL, PHYSICAL & ENGINEERING SCIENCES

also be unravelled by drawing on the success of the Si work and differences in theoretically expected behaviour.

This work has been supported by the Robert A. Welch Foundation and grants for U.S./European collaboration from NATO and the U.S. National Science Foundation.

References

Bech-Nielsen, B., Bonde-Nielsen, K. & Byberg, J. R. 1994 *Mater. Sci. Forum* **143-147**, 909.

Chow, K. H., *et al.* 1993 *Phys. Rev.* B **47**, 16004.

Chow, K. H., *et al.* 1994*a* *Hyp. Interact.* **86**, 693.

Chow, K. H., *et al.* 1994*b* *Phys. Rev.* B. **50**, 8918.

Estle, T. L., Estreicher, S. K. & Marynick, D. S. 1986 *Hyp. Interact.* **32**, 637.

Estle, T. L., Estreicher, S. K. & Marynick, D. S. 1987 *Phys. Rev. Lett.* **58**, 1547.

Estreicher, S. K. 1987 *Phys. Rev.* B **32**, 9122.

Gorelkinski, Yu. V. & Nevinnyi, N. N. 1992 *Physica* B **170**, 155.

Hitti, B., *et al.* 1994 *Hyp. Interact.* **86**, 673.

Holm, B., Bonde-Nielsen, K. & Bech-Nielsen, B. 1991 *Phys. Rev. Lett.* **66**, 2360.

Kiefl, R. F., *et al.* 1988 *Phys. Rev. Lett.* **60**, 224.

Kiefl, R. F. & Estle, T. L. 1990 In *Hydrogen in semiconductors* (ed. J. Pankove & N. M. Johnson), p. 547. New York: Academic.

Kreitzman, S. R., *et al.* 1994 *Phys. Rev.* B. (Submitted.)

Lichti, R. L., *et al.* 1994*a* *Hyp. Interact.* **86**, 711.

Lichti, R. L., *et al.* 1994*b* *Mater. Sci. Forum* **143–147**, 915.

Lichti, R. L., *et al.* 1992 *Mater. Sci. Forum* **83–87**, 1115.

Myers, S. M., *et al.* 1992 *Rev. mod. Phys.* **64**, 552.

Patterson, B. D. 1988 *Rev. mod. Phys.* **60**, 69.

Simmler, H., *et al.* 1992 *Mater. Sci. Forum* **83–87**, 1121.

PHILOSOPHICAL TRANSACTIONS OF THE ROYAL SOCIETY A MATHEMATICAL, PHYSICAL & ENGINEERING SCIENCES